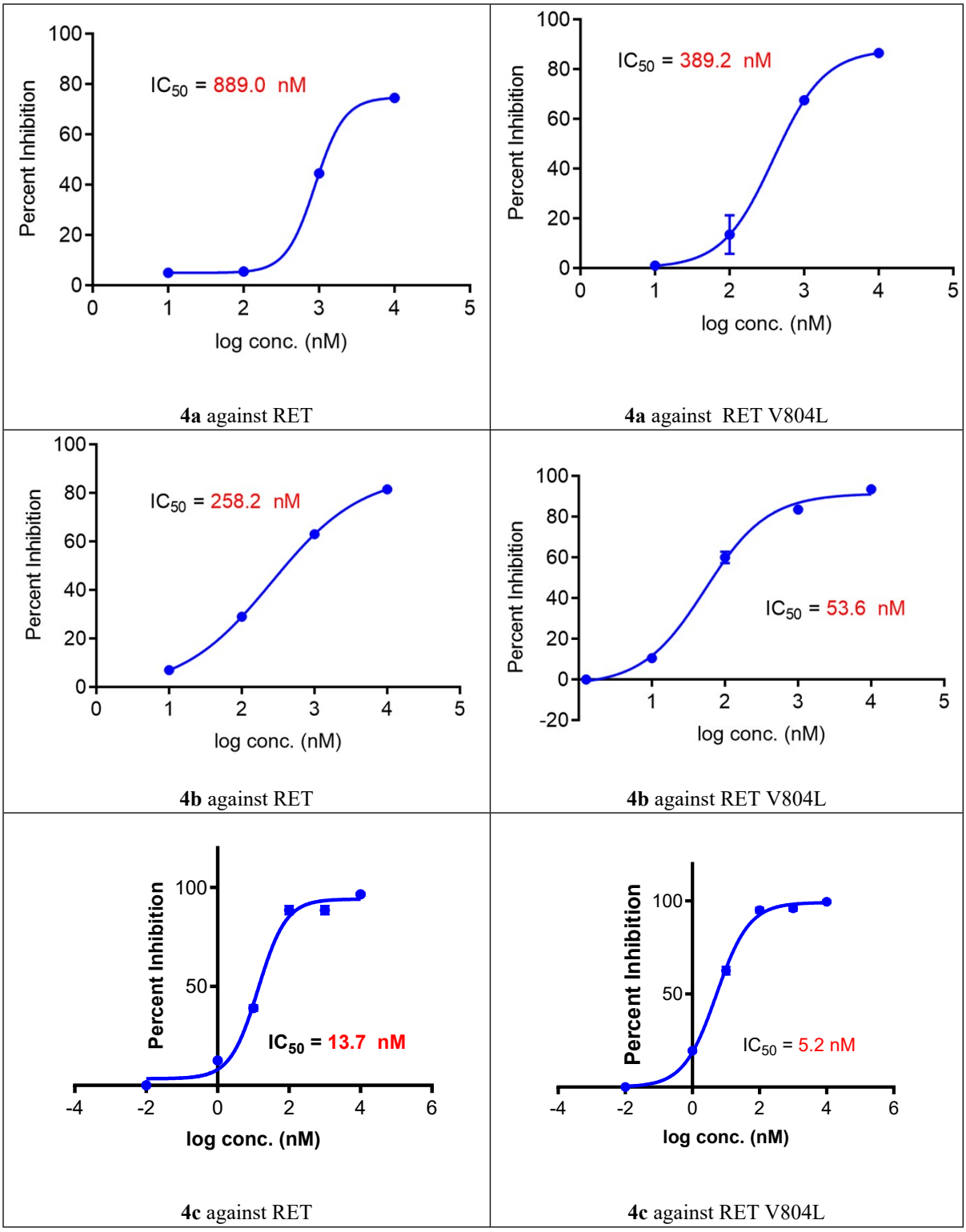

Figure S1. Dose response curves of compounds **4a-c** against **RET** and **RET V804L**

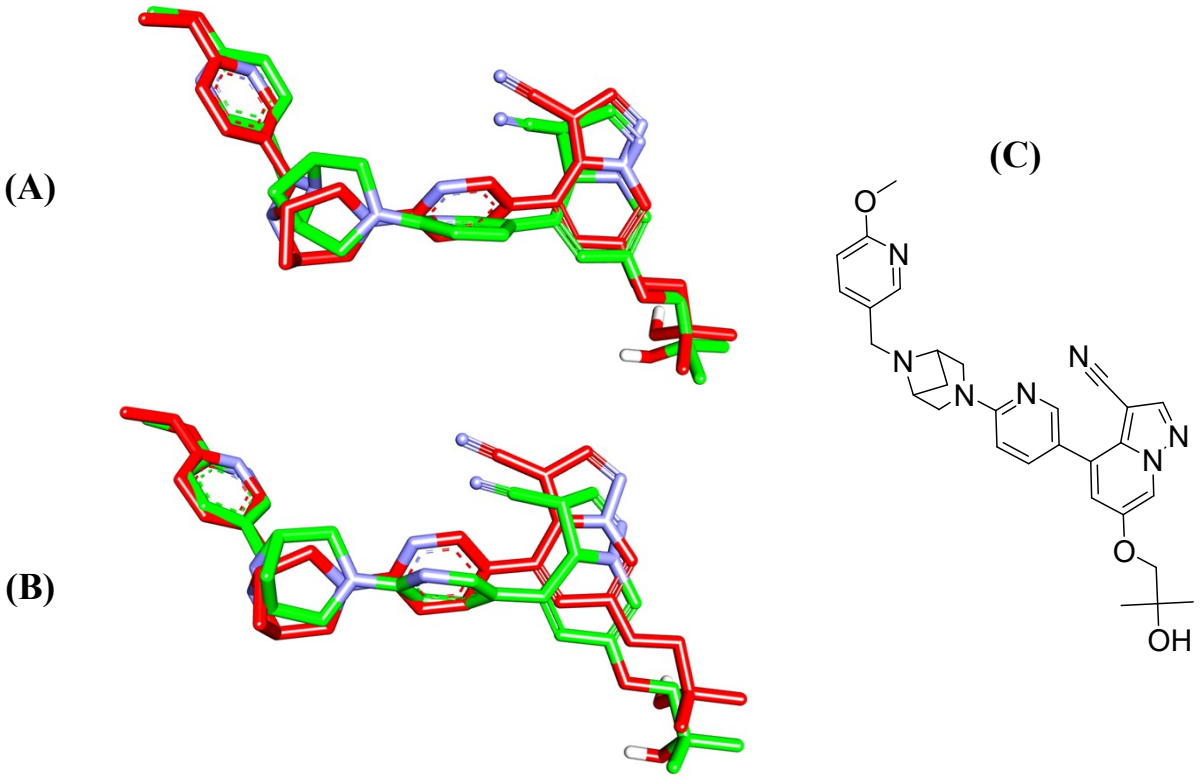

Figure S2-A: Docking veracity. Comparison between docked poses (green) and crystallographic bound poses (red) of selpercatinib: (**A)** within wild type RET kinase (PDB code: 7JU6), **(B)** within a homology model of RET kinase produced by manually replacing Val804 with Leu804. **(C)** The chemical structure of selpercatinib (anti-RET IC_{50} = 0.4 to 531 nM).

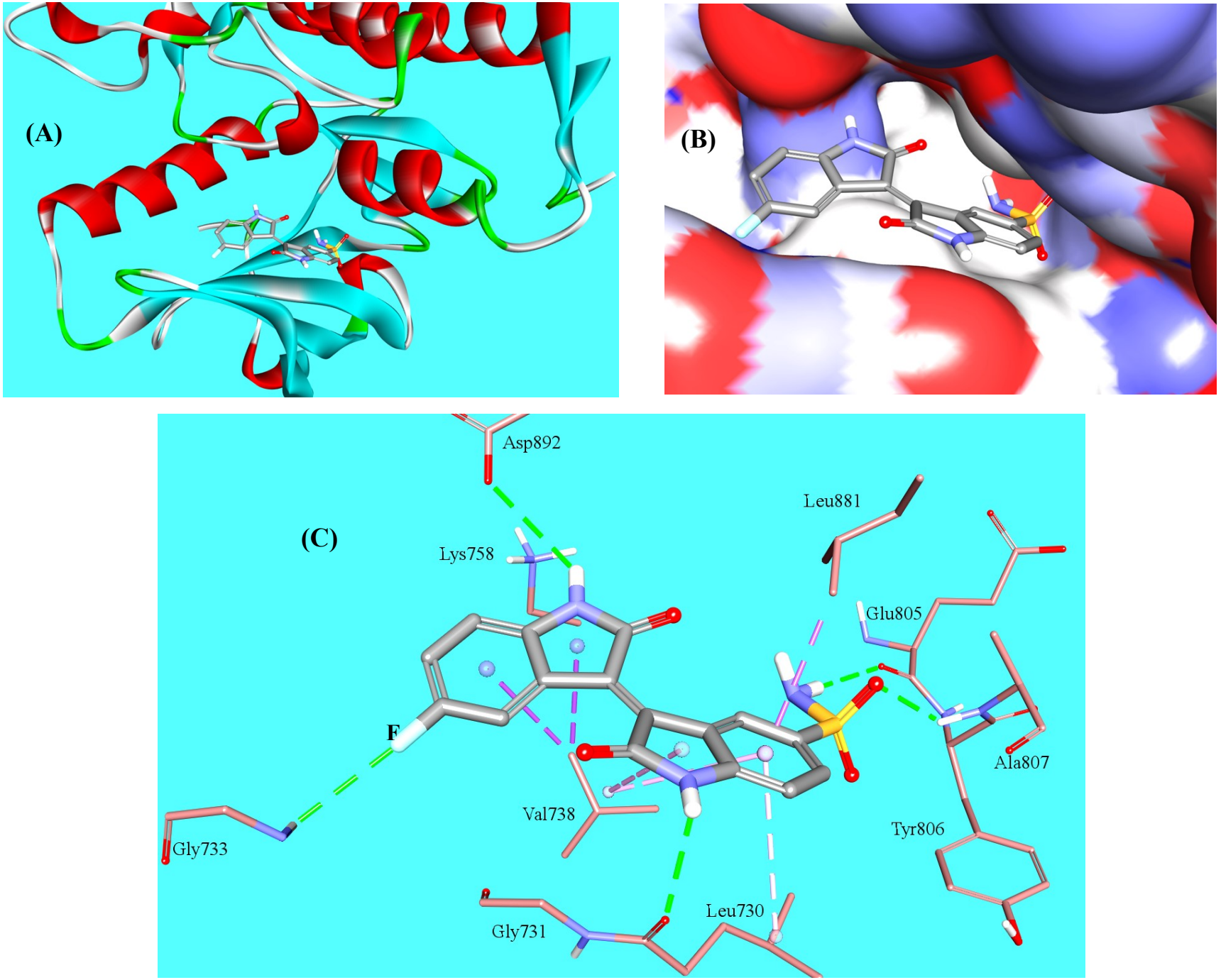

Figure S2-B: **4a** docked into wild type RET kinase. **(A)** Panoramic view of the docked complex. **(B)** The docked ligand within the binding pocket covered by Connolly surface solvent accessible surface. **(C)** Detailed view of the docked complex showing interaction details. Hydrogen bonds are represented as green dotted lines, hydrophobic interactions are represented as white, pink or light-pink dotted lines.

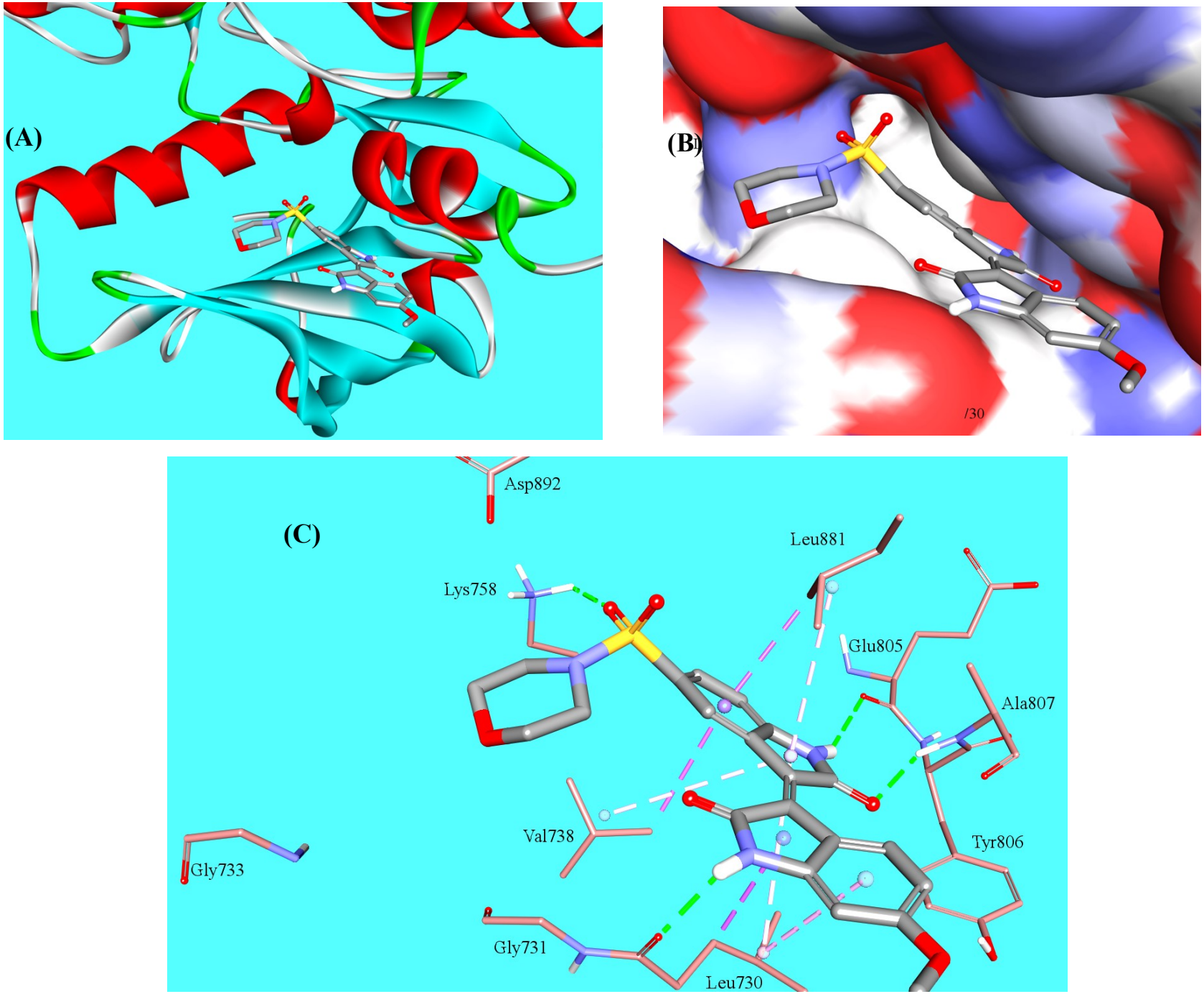

Figure S2-C: **4b** docked into wild type RET kinase. **(A)** Panoramic view of the docked complex. **(B)** The docked ligand within the binding pocket covered by Connolly surface solvent accessible surface. **(C)** Detailed view of the docked complex showing interaction details. Hydrogen bonds are represented as green dotted lines, hydrophobic interactions are represented as white, pink or light-pink dotted lines.

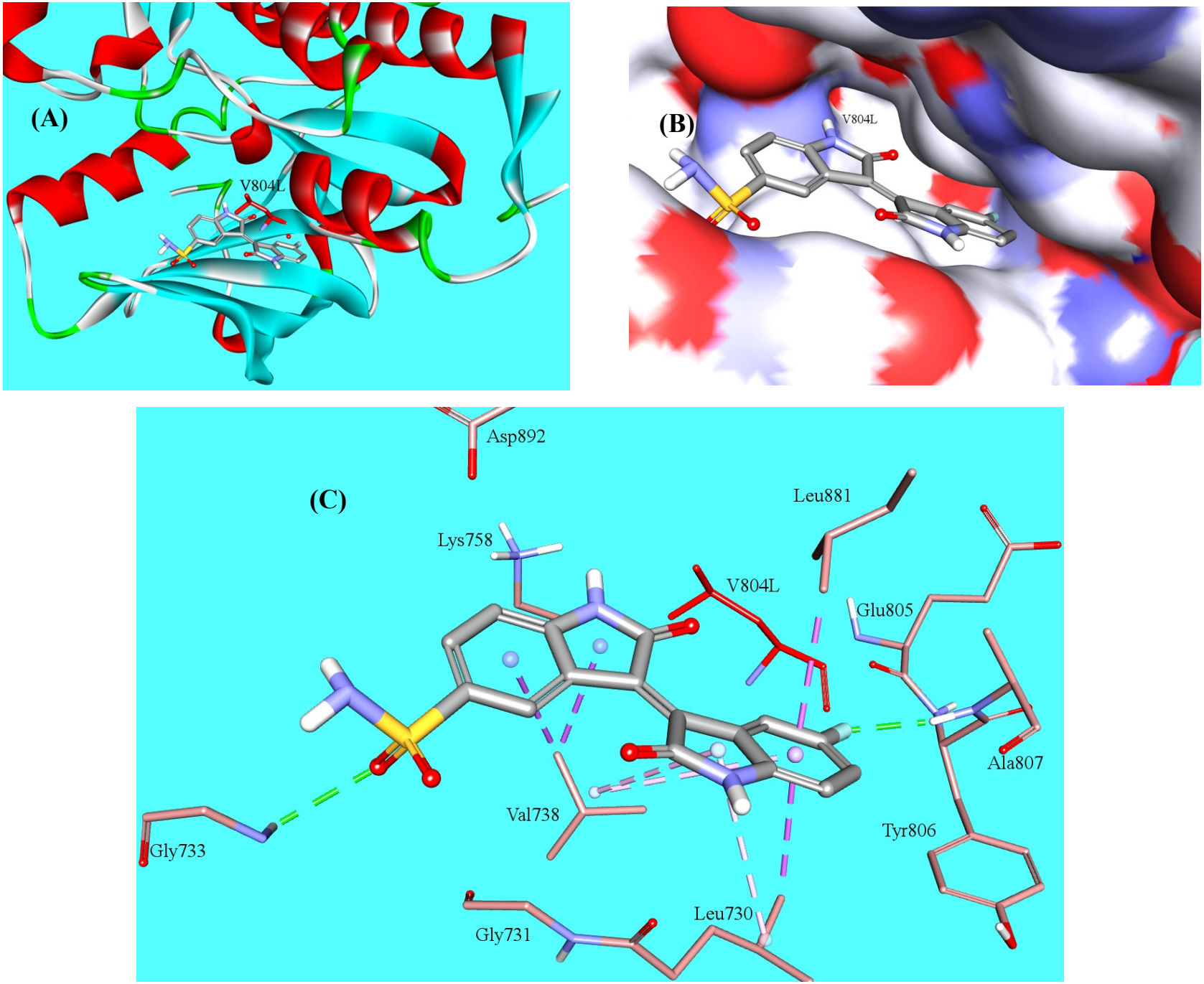

Figure S2-D: **4a** docked into V804L RET kinase. **(A)** Panoramic view of the docked complex. **(B)** The docked ligand within the binding pocket covered by Connolly surface solvent accessible surface. **(C)** Detailed view of the docked complex showing interaction details. Hydrogen bonds are represented as green dotted lines; hydrophobic interactions are represented as white, pink or light-pink dotted lines. The V804L mutation site is shown in red.

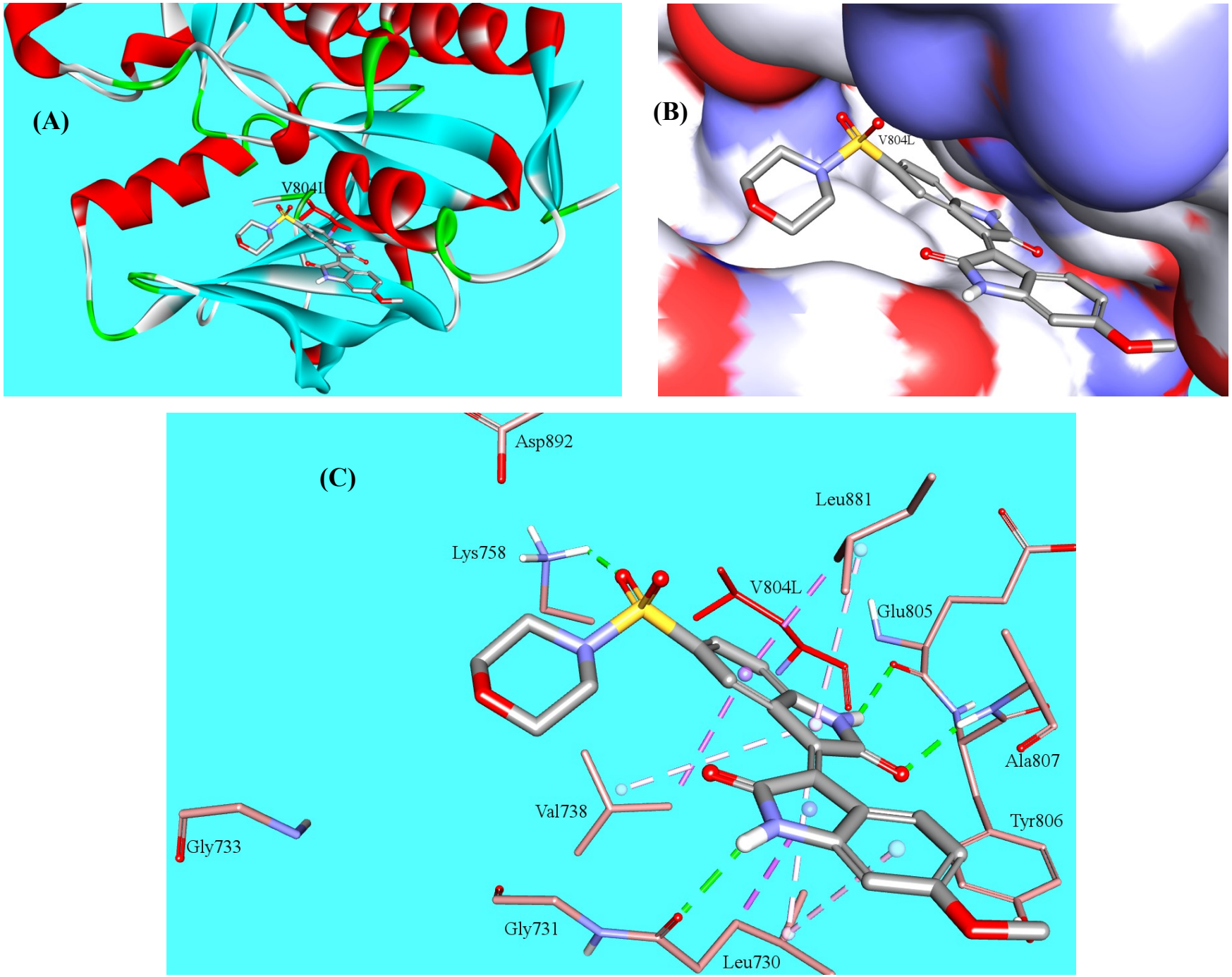

Figure S2-E: **4b** docked into V804L RET kinase. **(A)** Panoramic view of the docked complex. **(B)** The docked ligand within the binding pocket covered by Connolly surface solvent accessible surface. **(C)** Detailed view of the docked complex showing interaction details. Hydrogen bonds are represented as green dotted lines; hydrophobic interactions are represented as white, pink or light-pink dotted lines. The V804L mutation site is shown in red.

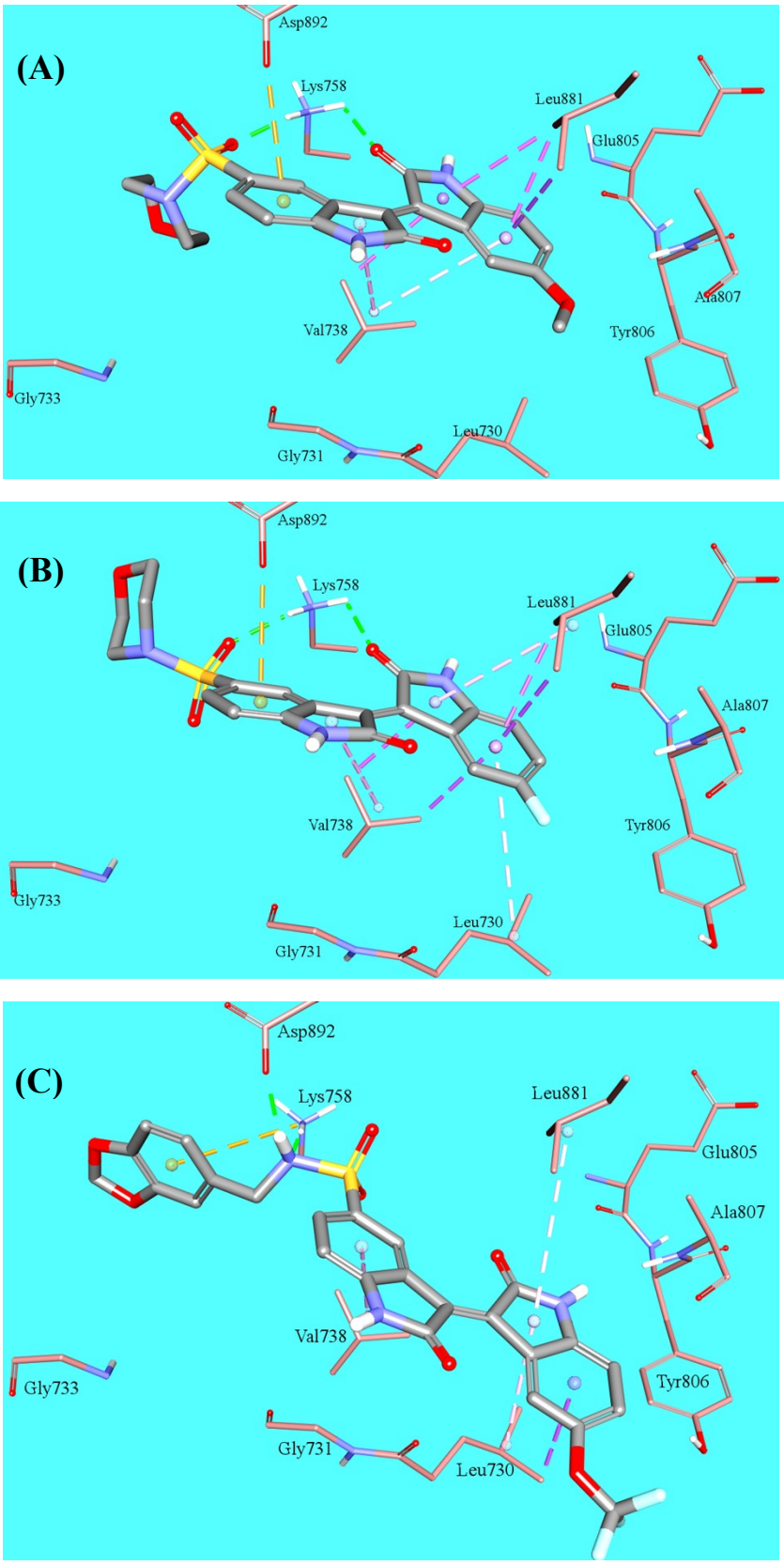

Figure S3: Docking of **(A) 4d**, **(B) 4e** and **(C) 4f** into wild type RET kinase. Hydrogen bonds are represented as green dotted lines, hydrophobic interactions are represented as white, pink or light-pink dotted lines. Ionic-π stacking interactions are represented by light-orange dotted lines.

Table S1. Enthalpic gains upon binding of selected compounds as estimated from CDOCKER interaction energy (Kcal /mol)

Compound	Docking into wild-type RET	Docking into mutated RET V804L
4a	38.2	36.9
4b	48.3	50.8
4c	44.4	46.2
Selpercatinib	59.7	61.2

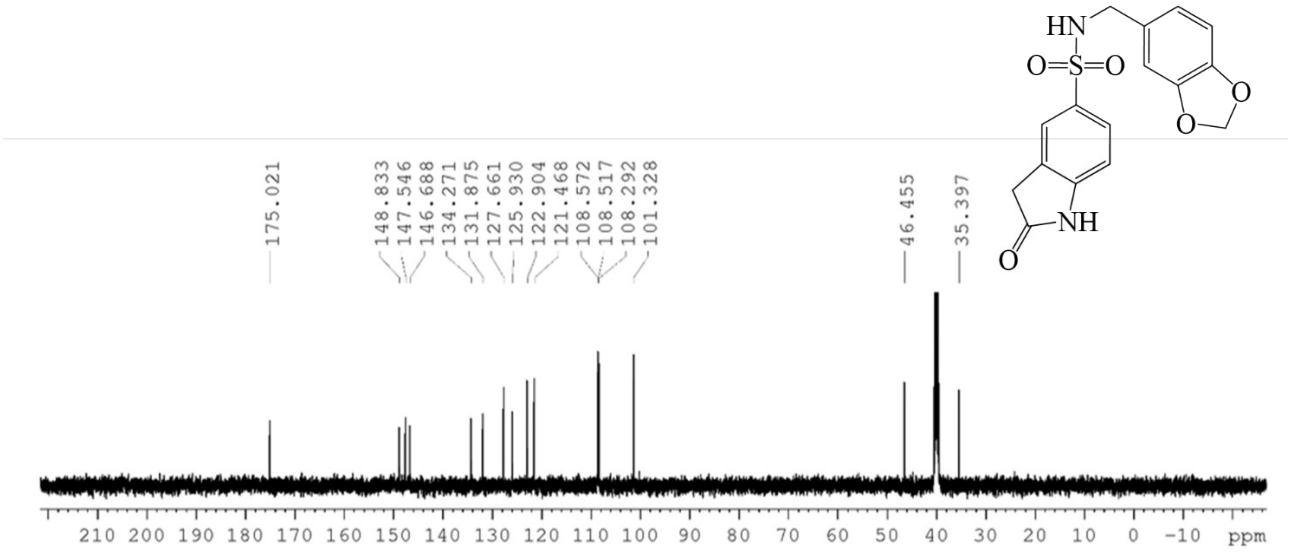

Figure S4 A: ^{13}C-NMR spectrum of compound [**2d**] DMSO

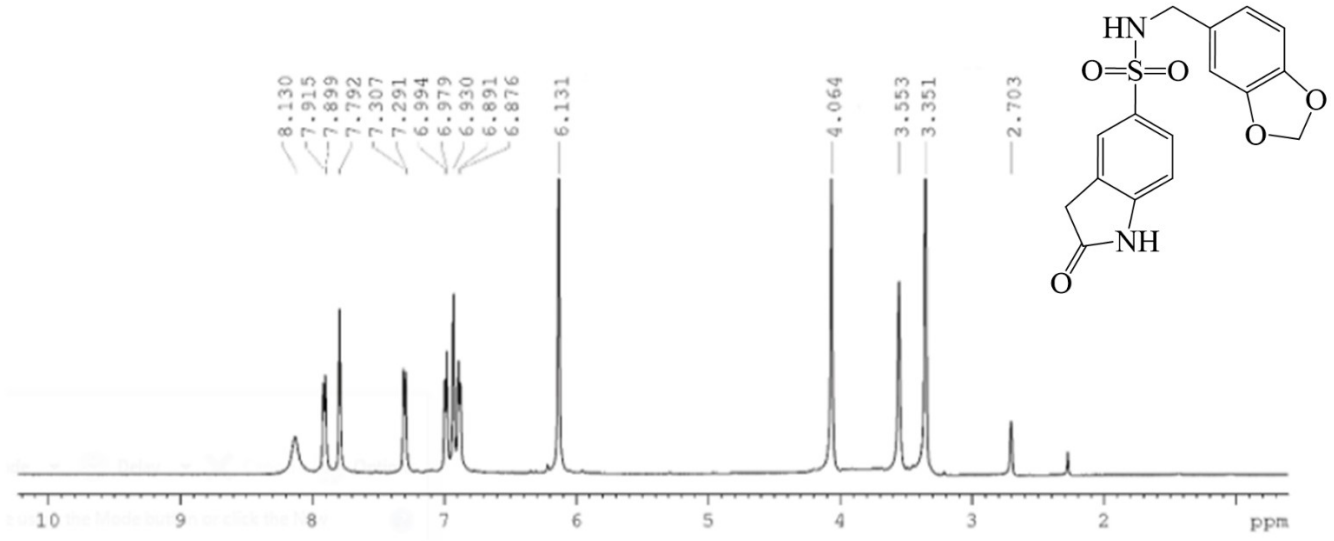

Figure S4 b: [1]H-NMR spectrum of compound [**2d**] DMSO

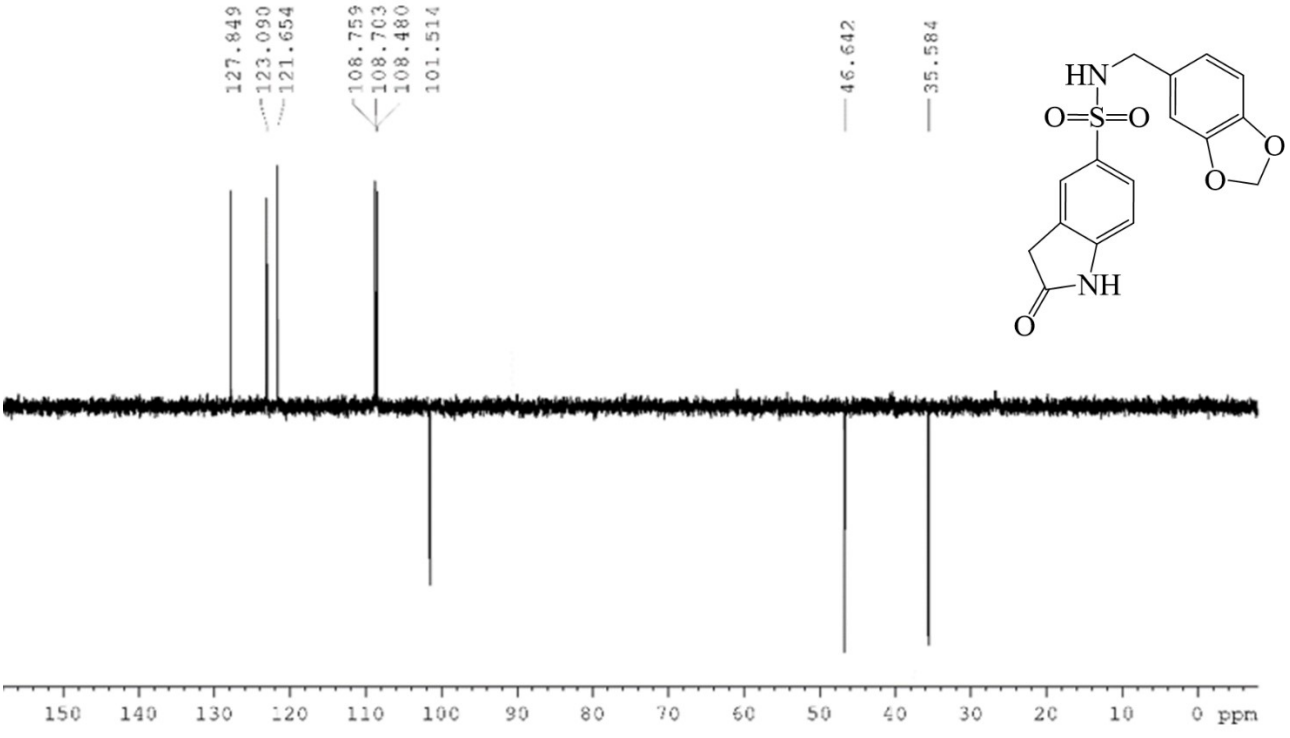

Figure S4 c: [13]C-NMR dept 135 spectra of compound [**2d**] DMSO

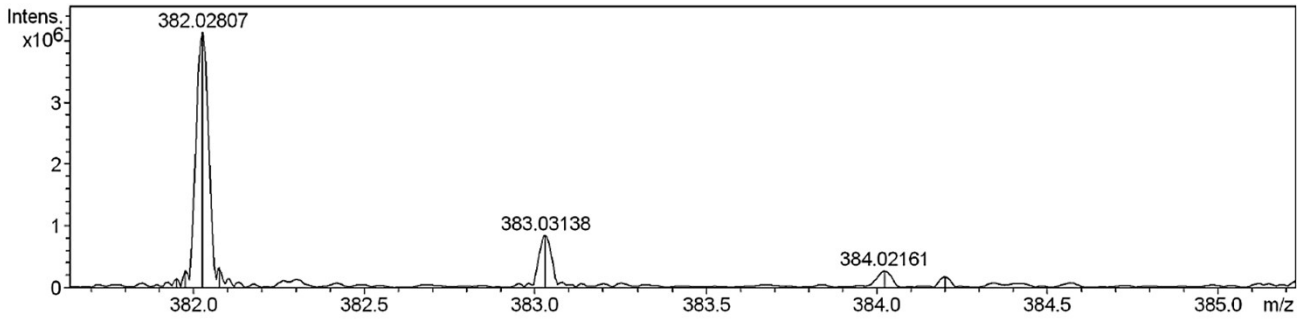

Figure S5: Mass spectroscopy chart of (E)-5'-fluoro-2,2'-dioxo-[3,3'-biindolinylidene]-5-sulfonamide (**4a**)

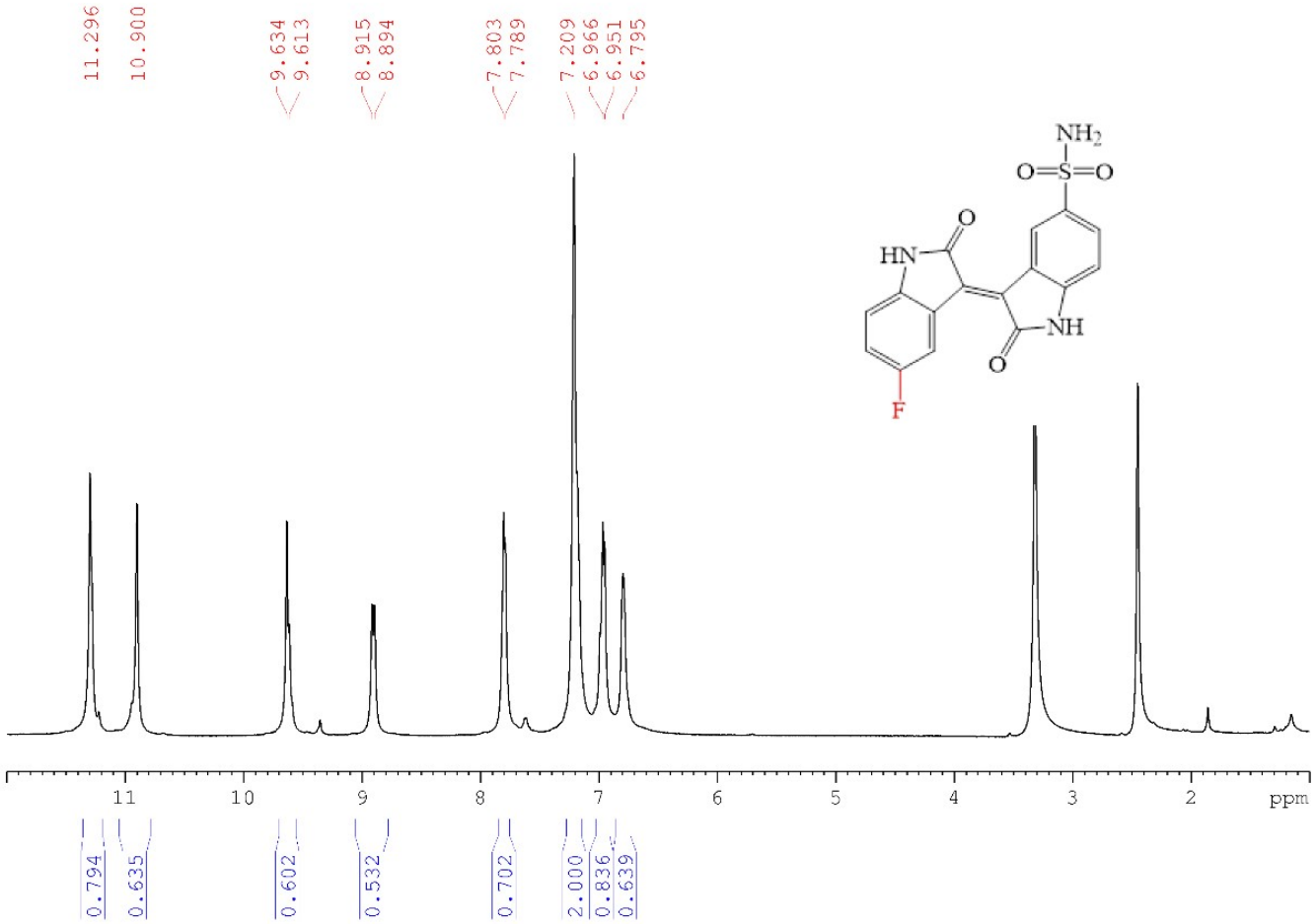

Figure S5: (E)-5'-fluoro-2,2'-dioxo-[3,3'-biindolinylidene]-5-sulfonamide (**4a**)

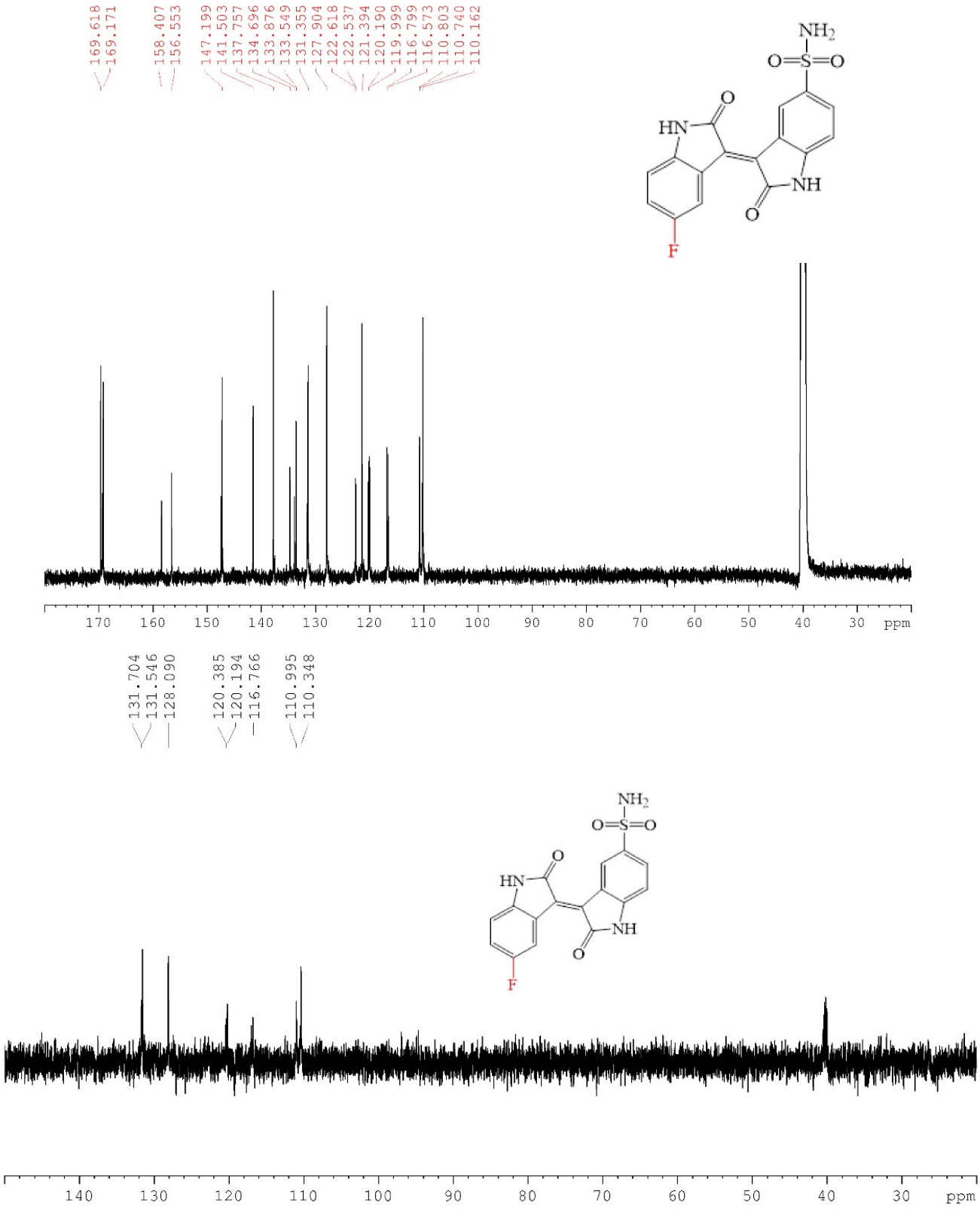

Figure S5: (E)-5'-fluoro-2,2'-dioxo-[3,3'-biindolinylidene]-5-sulfonamide (**4a**)

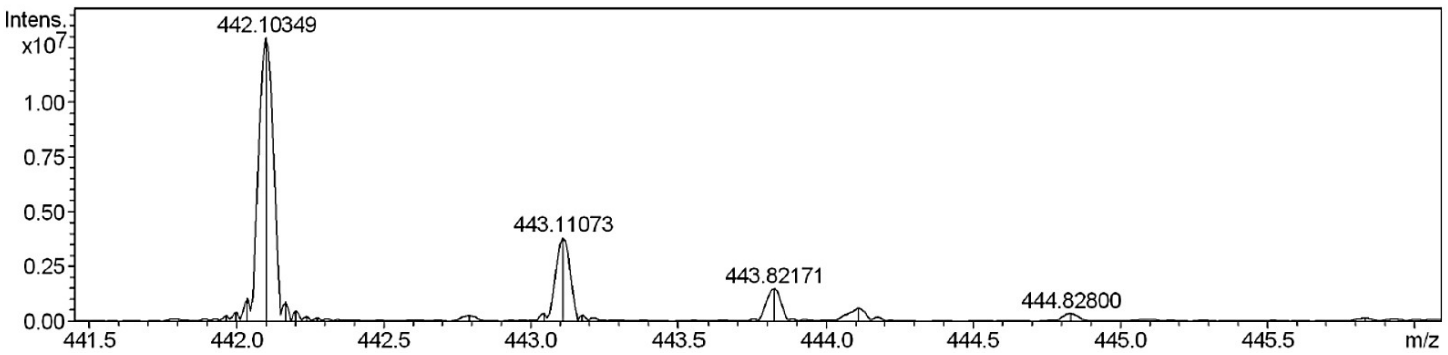

Figure S6 Mass spectroscopy chart of (E)-6'-methoxy-5-(morpholinosulfonyl)-[3,3'-biindolinylidene]-2,2'-dione (**4b**)

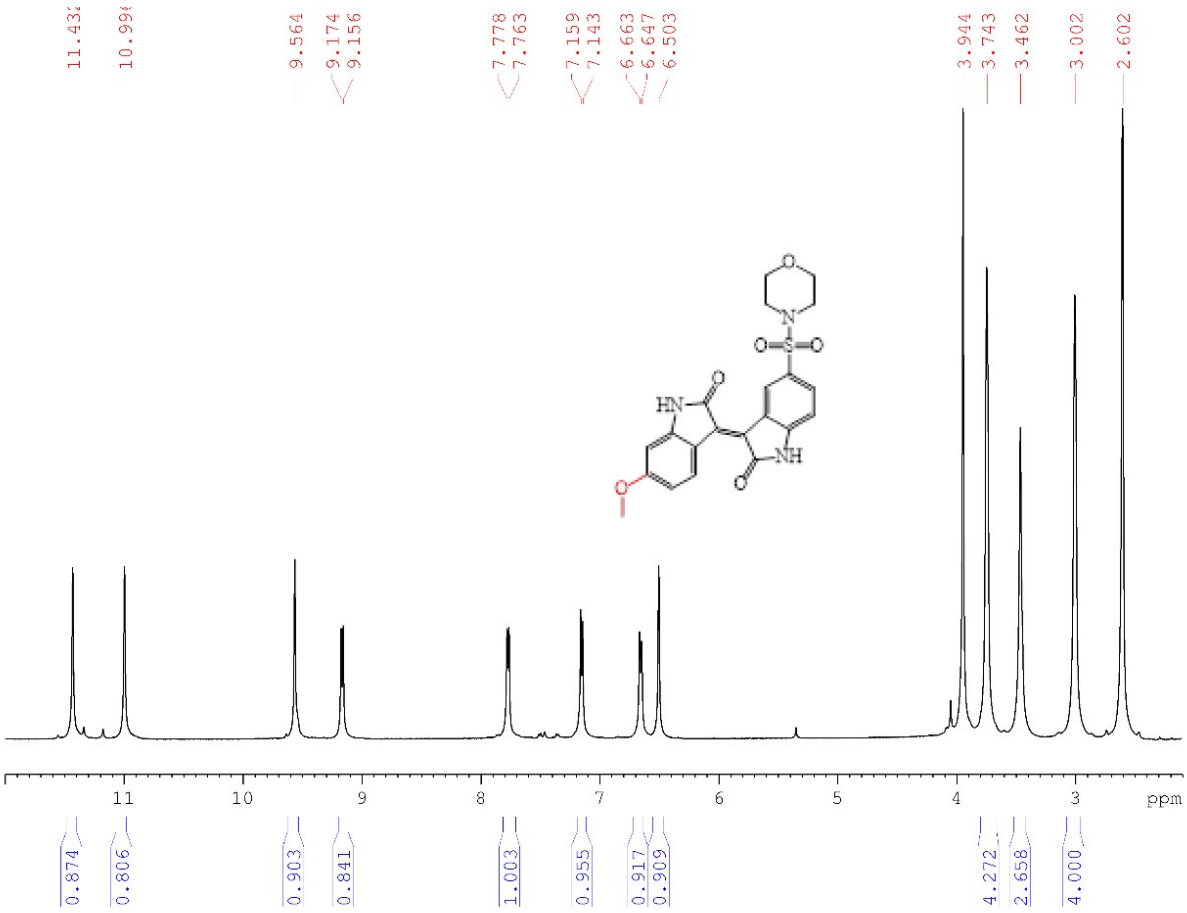

Figure S6 (E)-6'-methoxy-5-(morpholinosulfonyl)-[3,3'-biindolinylidene]-2,2'-dione (**4b**)

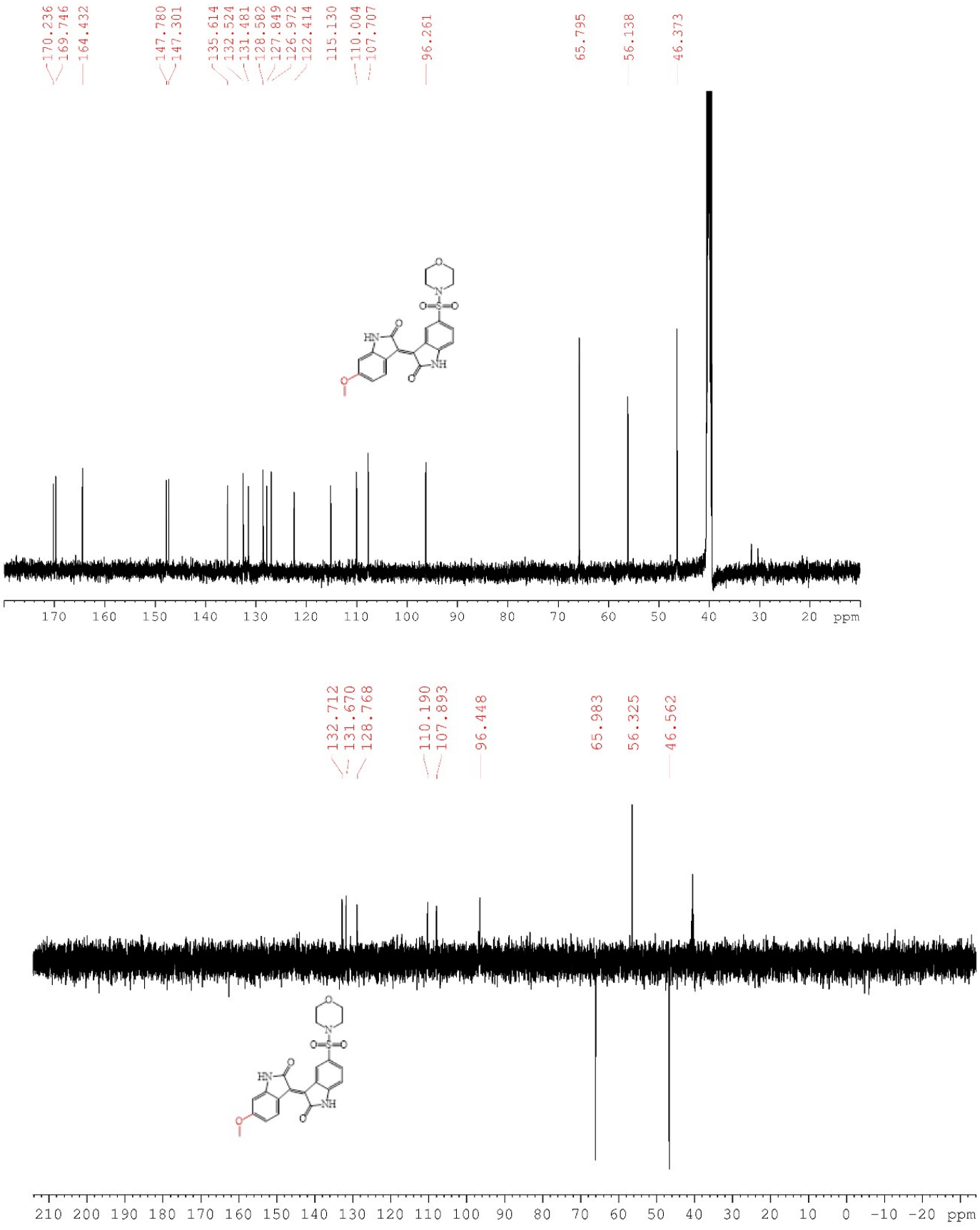

Figure S6 (E)-6'-methoxy-5-(morpholinosulfonyl)-[3,3'-biindolinylidene]-2,2'-dione (**4b**)

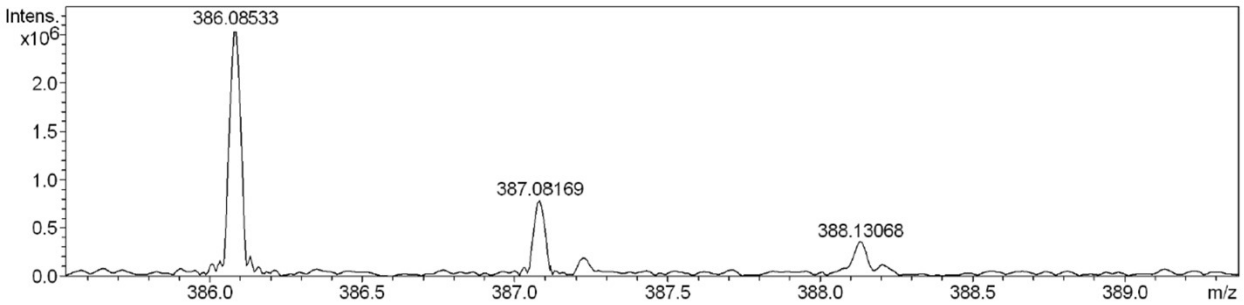

Figure S7 Mass spectroscopy chart of (E)-6'-methoxy-N-methyl-2,2'-dioxo-[3,3'-biindolinylidene]-5-sulfonamide (**4c**)

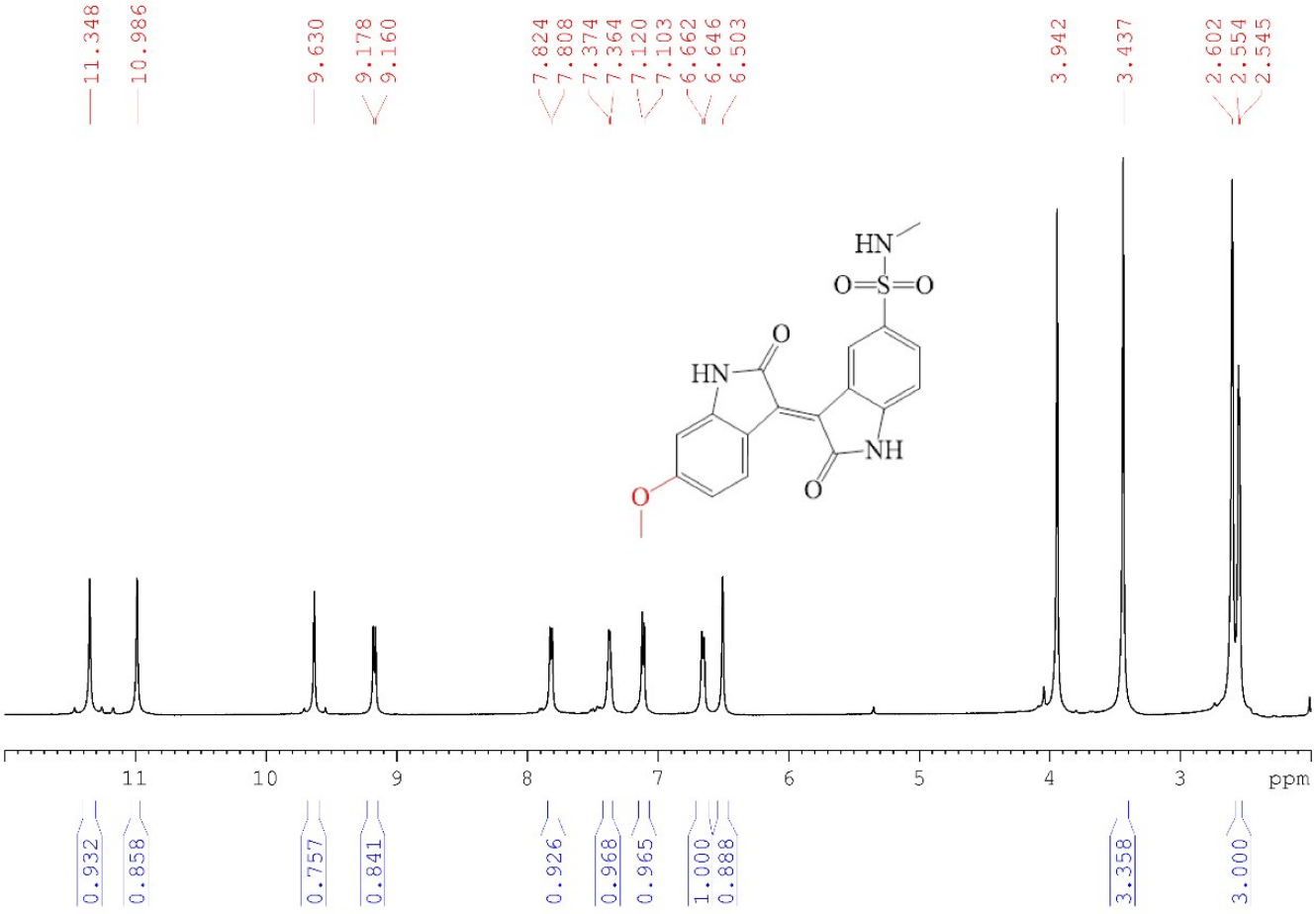

Figure S7 (E)-6'-methoxy-N-methyl-2,2'-dioxo-[3,3'-biindolinylidene]-5-sulfonamide (**4c**)

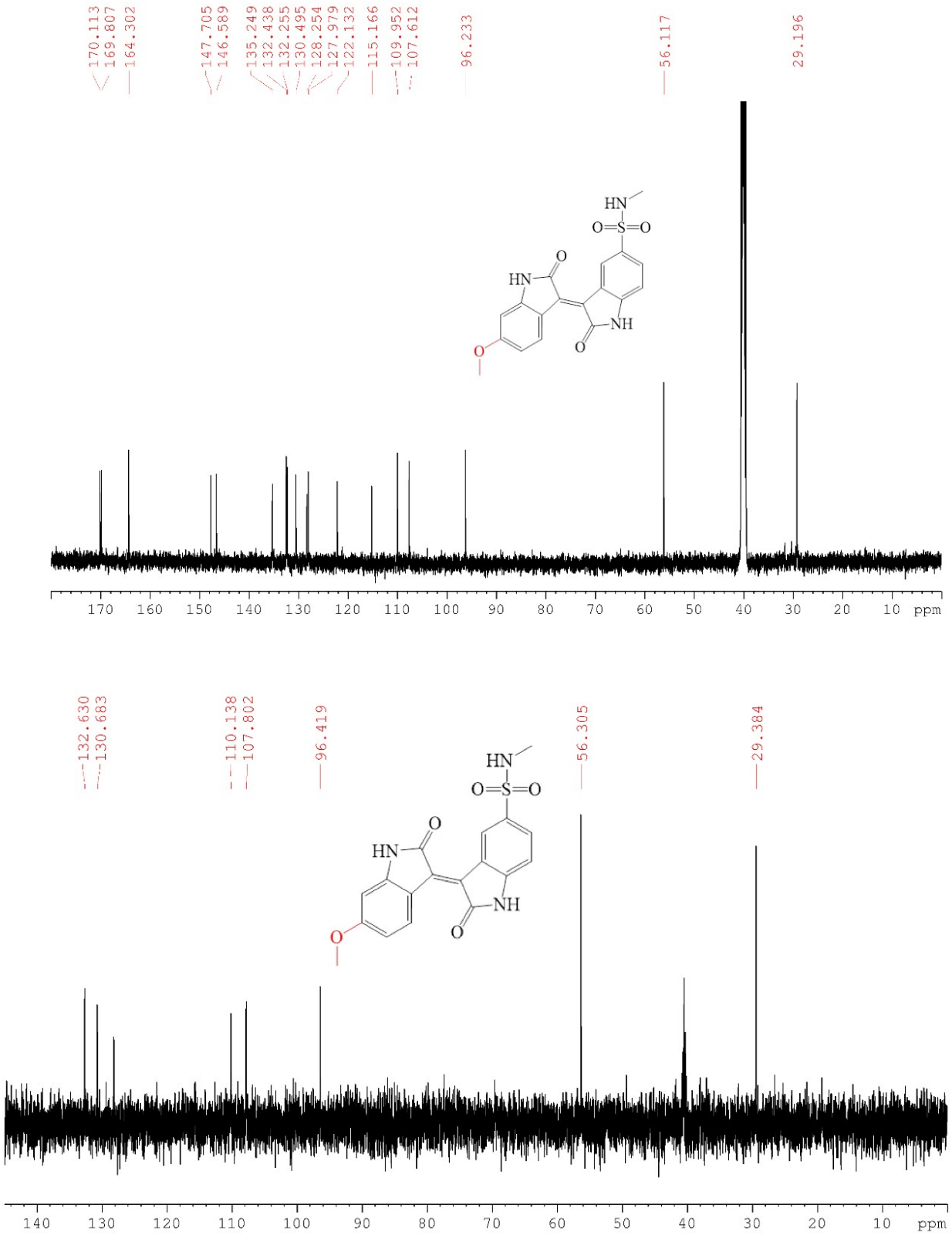

Figure S7 (E)-6'-methoxy-N-methyl-2,2'-dioxo-[3,3'-biindolinylidene]-5-sulfonamide (**4c**)

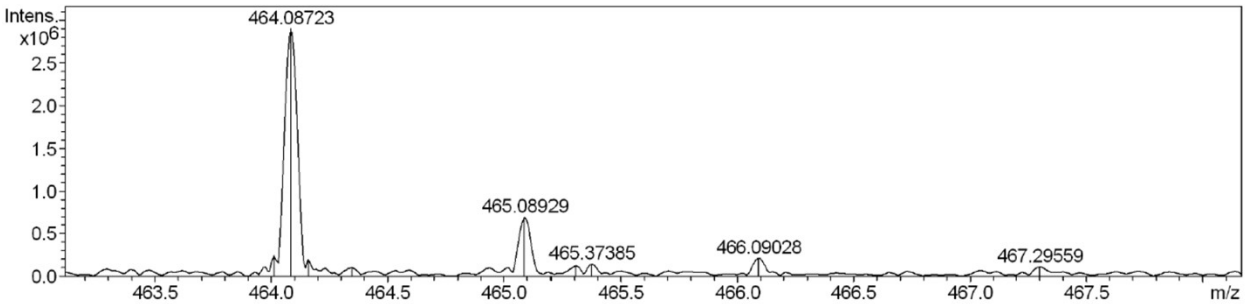

Figure S8 Mass spectroscopy chart of (E)-5-methoxy-5'-(morpholinosulfonyl)-[3,3'-biindolinylidene]-2,2'-dione (**4d**)

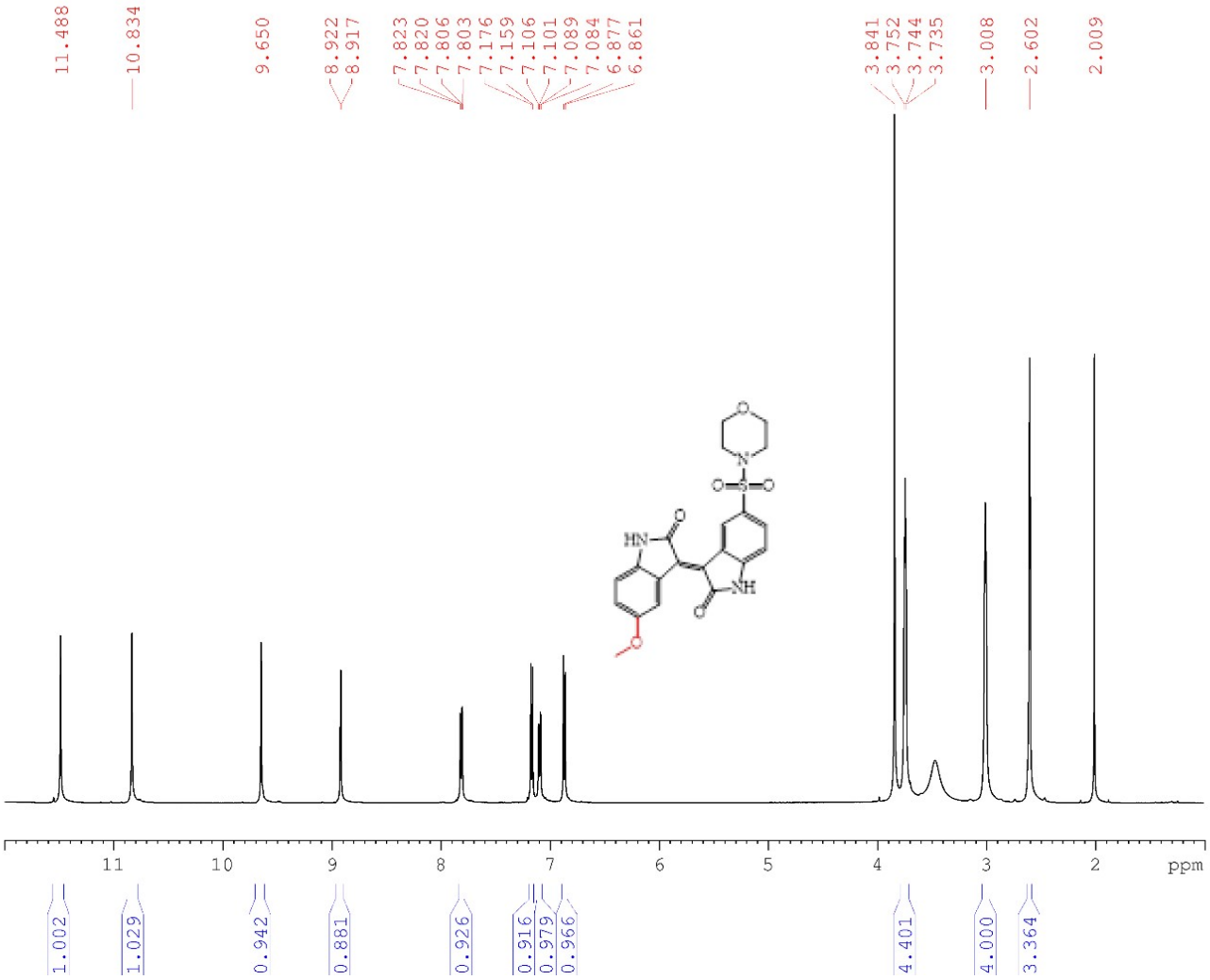

Figure S8 (E)-5-methoxy-5'-(morpholinosulfonyl)-[3,3'-biindolinylidene]-2,2'-dione (**4d**)

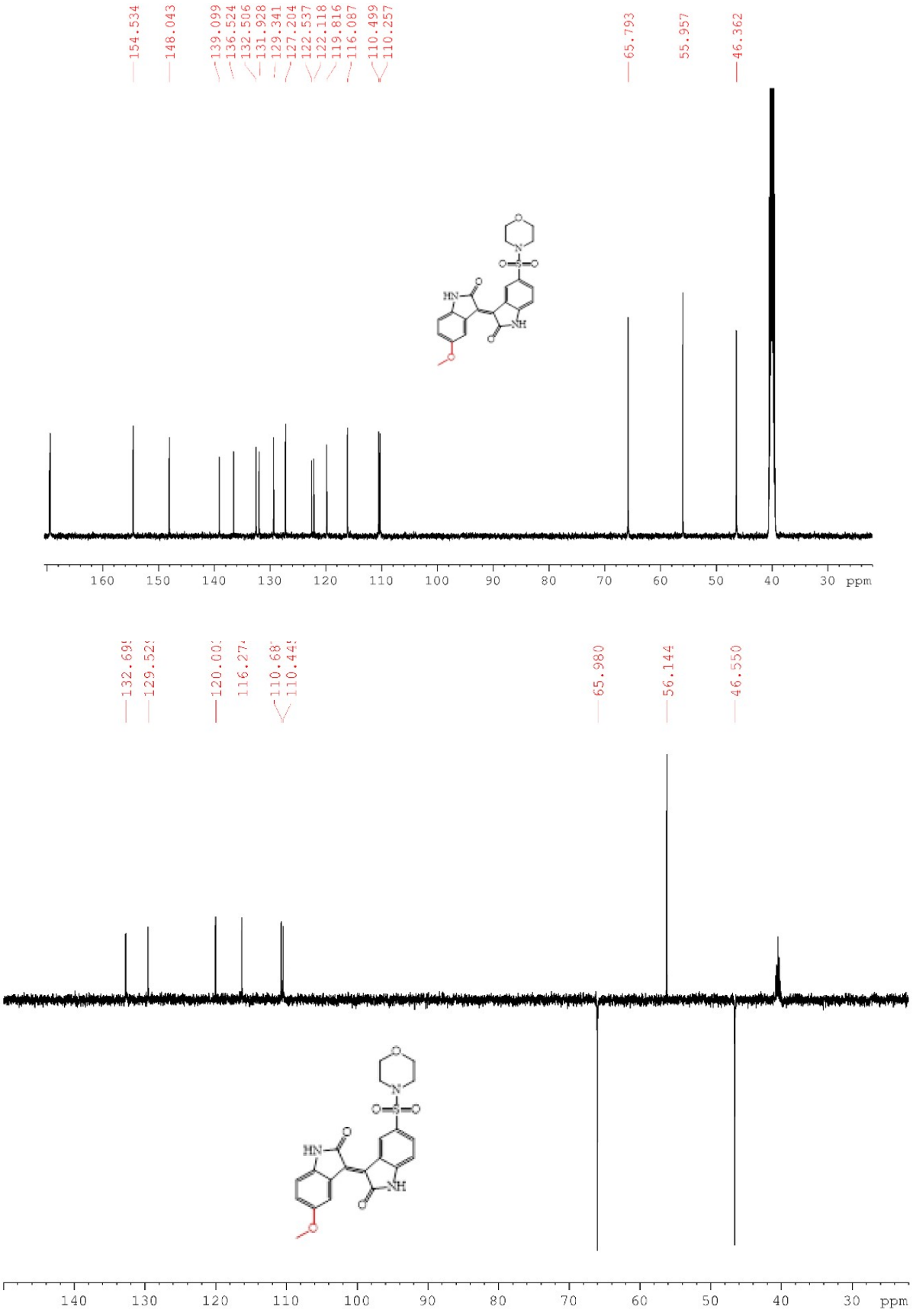

Figure S8 (E)-5-methoxy-5'-(morpholinosulfonyl)-[3,3'-biindolinylidene]-2,2'-dione (**4d**)

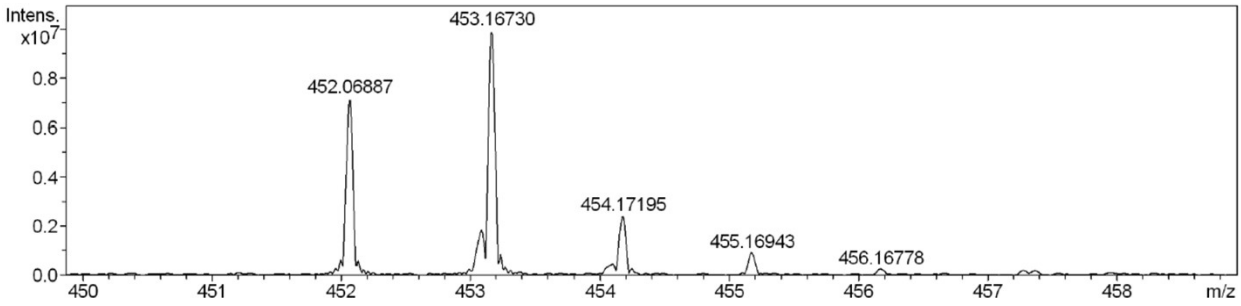

Figure S9 Mass spectroscopy chart of (E)-5-fluoro-5'-(morpholinosulfonyl)-[3,3'-biindolinylidene]-2,2'-dione (**4e**)

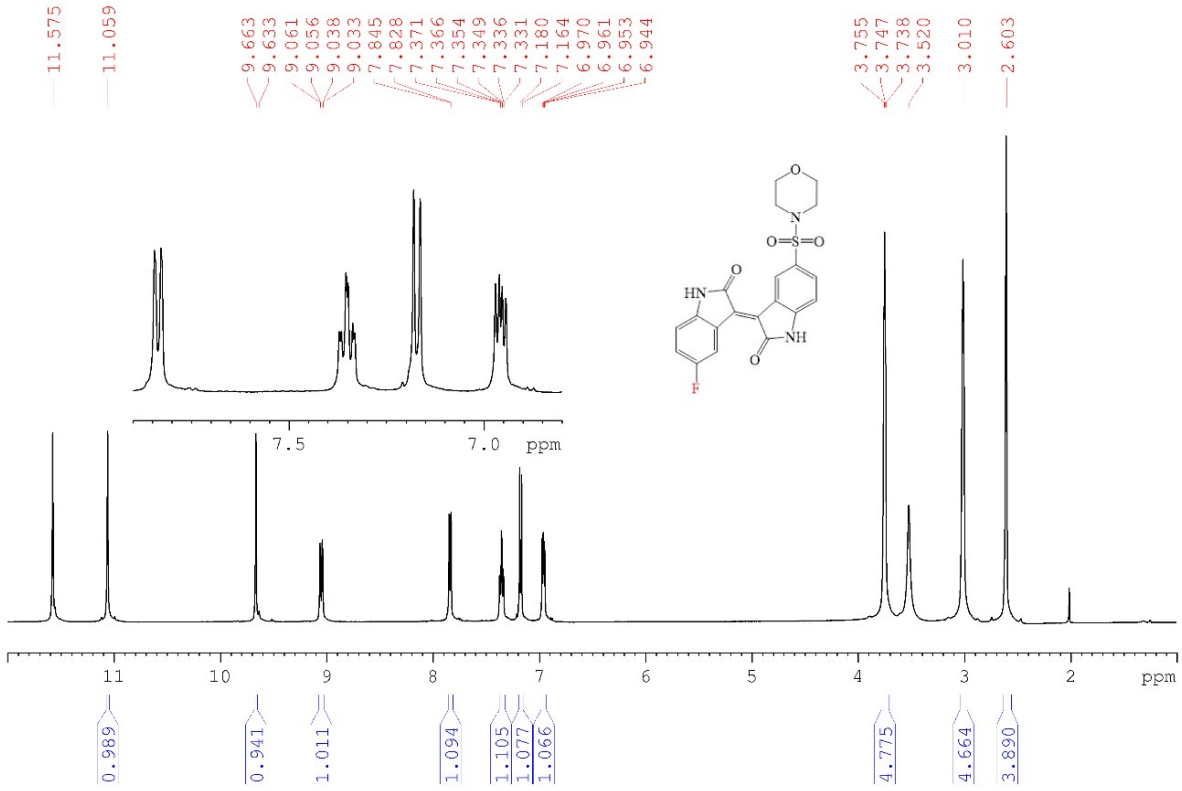

Figure S9 (E)-5-fluoro-5'-(morpholinosulfonyl)-[3,3'-biindolinylidene]-2,2'-dione (**4e**)

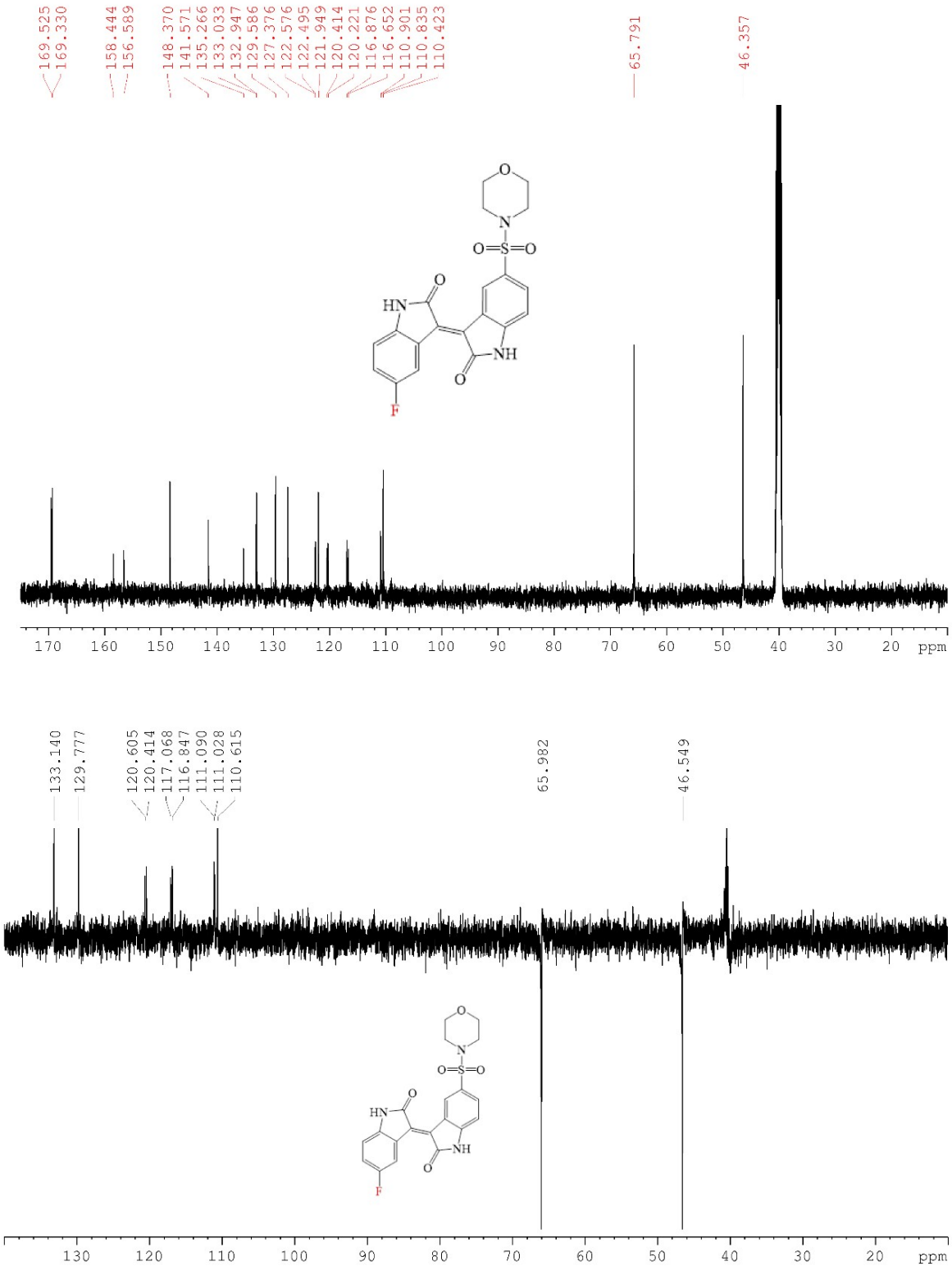

Figure S9 (E)-5-fluoro-5'-(morpholinosulfonyl)-[3,3'-biindolinylidene]-2,2'-dione (**4e**)

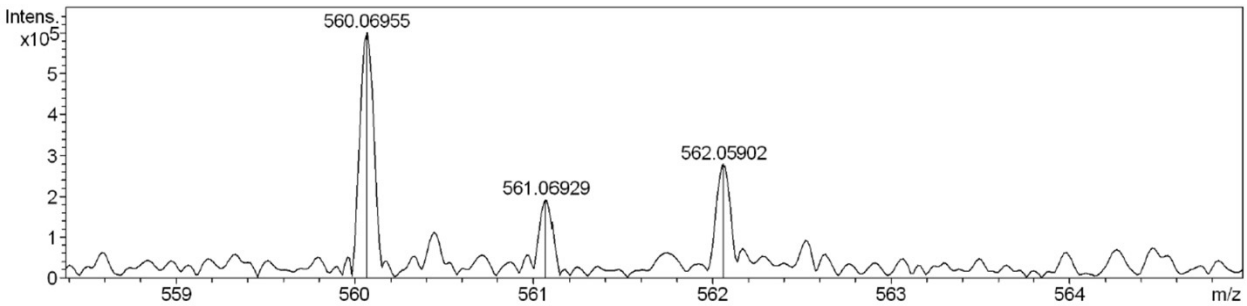

Figure S10 Mass spectroscopy chart of (E)-N-(benzo[d][1,3]dioxol-5-ylmethyl)-2,2'-dioxo-5'-(trifluoromethoxy)-[3,3'-biindolinylidene]-5-sulfonamide (**4f**)

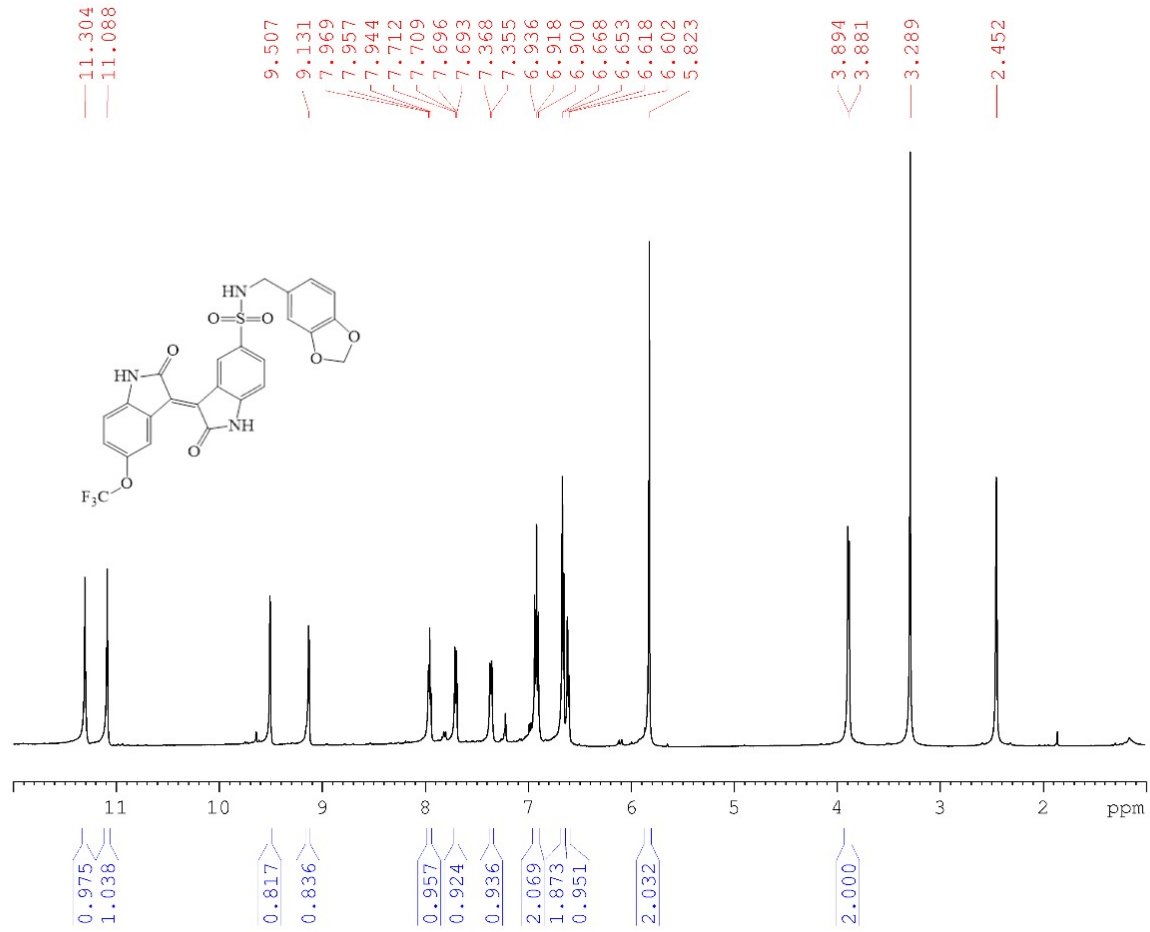

Figure S10 (E)-N-(benzo[d][1,3]dioxol-5-ylmethyl)-2,2'-dioxo-5'-(trifluoromethoxy)-[3,3'-biindolinylidene]-5-sulfonamide (**4f**)

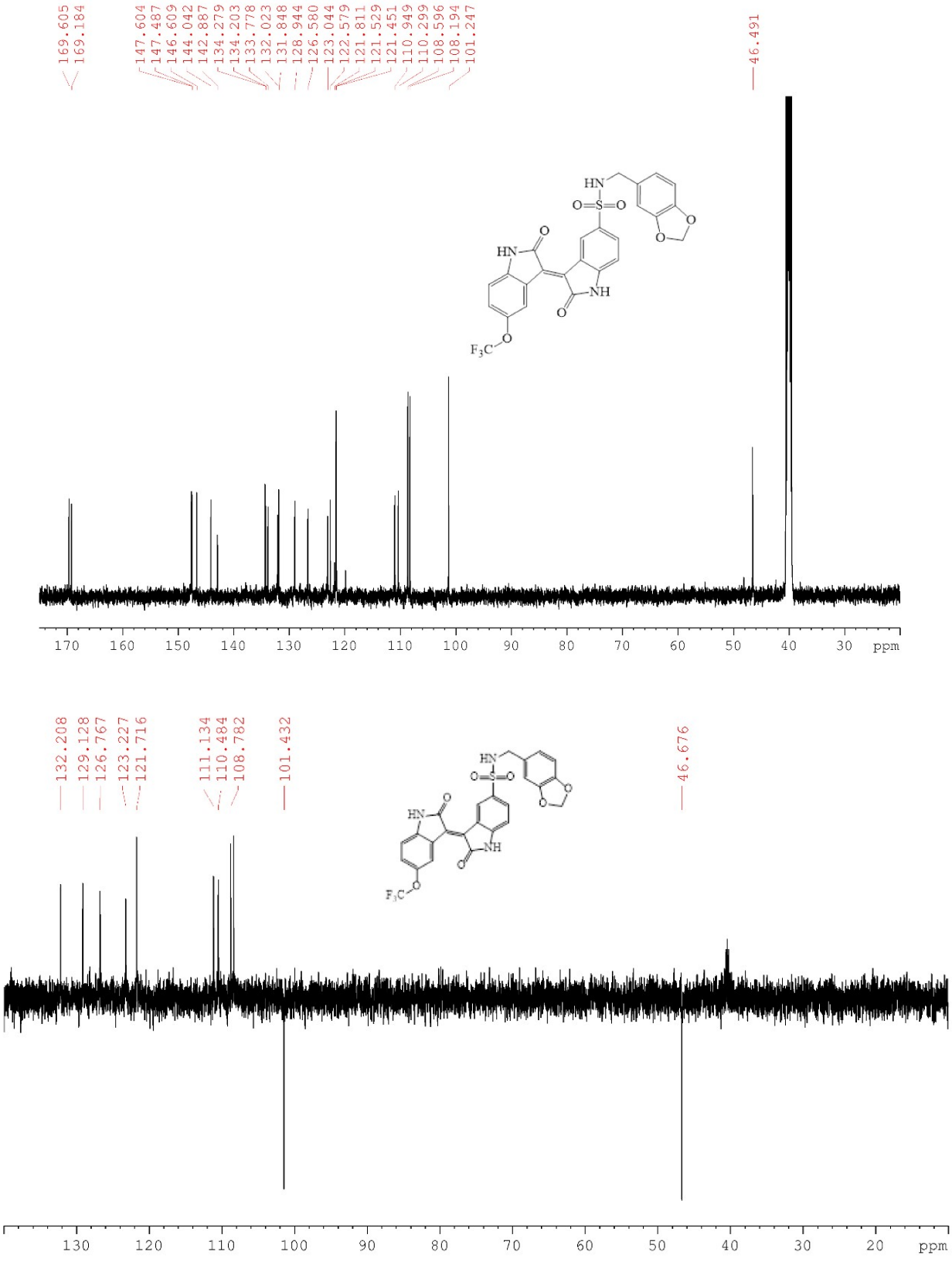

Figure S10 (E)-N-(benzo[d][1,3]dioxol-5-ylmethyl)-2,2'-dioxo-5'-(trifluoromethoxy)-[3,3'-biindolinylidene]-5-sulfonamide (**4f**)